DOI: 10.1002/cbic.200700738

Covalent Linkage Mediates Communication between ACP and TE Domains in Modular Polyketide Synthases

Lucky Tran,[a] Manuela Tosin,[b] Jonathan B. Spencer,[b] Peter F. Leadlay,[a] and Kira J. Weissman*[a, c]

Polyketide natural products such as erythromycin A and epothilone are assembled on multienzyme polyketide synthases (PKSs), which consist of modular sets of protein domains. Within these type I systems, the fidelity of biosynthesis depends on the programmed interaction among the multiple domains within each module, centered around the acyl carrier protein (ACP). A detailed understanding of interdomain communication will therefore be vital for attempts to reprogram these pathways by genetic engineering. We report here that the interaction between a representative ACP domain and its downstream thioesterase (TE) is mediated largely by covalent tethering through a short "linker" region, with only a minor energetic contribution from protein–protein molecular recognition. This finding helps explain in part the empirical observation that TE domains can function out of their normal context in engineered assembly lines, and supports the view that overall PKS architecture may dictate at least a subset of interdomain interactions.

Introduction

Polyketide secondary metabolites from bacteria are a valuable source of pharmaceuticals, agrochemicals, and veterinary agents.[1,2] Biosynthesis of these compounds is governed by enzyme complexes called polyketide synthases (PKSs), which catalyze a series of sequential condensation reactions of simple carboxylic acid precursors. PKSs are classified according to their architectural configurations: while type II PKS enzymes exist as discrete proteins,[3] type I PKSs are large multienzymes, in which the individual catalytic domains are covalently tethered together. A type I arrangement also occurs in the closely related fatty acid synthases (FASs) of animals.[4] Within type I PKSs, repeated sets of domains are grouped into modules, with each module catalyzing a different cycle of chain extension. For example, the 6-deoxyerythronolide B synthase (DEBS) responsible for biosynthesis of the antibiotic erythromycin A comprises six modules distributed among three gigantic multienzyme subunits: DEBS 1, DEBS 2, and DEBS 3 (Figure 1).[5,6] Each chain extension module houses three core domains—ketosynthase (KS), acyl transferase (AT), and acyl carrier protein (ACP)—which are required in order to select specific building blocks and to accomplish C–C bond formation. These functions can be optionally augmented by varying combinations of β-carbon-processing enzymes, including ketoreductase (KR), dehydratase (DH), and enoyl reductase (ER) domains. Chain release and cyclization is typically performed by a terminal thioesterase (TE) activity. As there is colinearity between the biosynthetic template and synthetic steps, predictions can be made for many elements of polyketide structure by examining the domain composition of the associated PKS. This modularity has also inspired an approach to generating novel polyketide analogues called combinatorial biosynthesis, in which specific portions of individual PKS are "mixed-and-matched" to produce hybrid synthases.[7]

A central component of PKS and FAS systems is the ACP, a small (~10 kDa) acidic protein or domain present in many metabolic pathways, where it plays a common role in tethering growing biosynthetic intermediates while they are extended and modified by the constituent enzymes. The structures of several discrete (so-called "type II") ACPs[8–12] and of the ACP_2 domain of DEBS[13] have been solved, and consist in each case of a distorted bundle of three or four α-helixes. Chain extension intermediates are attached to the ACP in thioester linkage via a 4′-phosphopantetheinyl (Ppant) moiety, a prosthetic group appended to a highly conserved serine residue at the base of helix αII. To accomplish a typical round of polyketide chain extension, the ACP interacts with all of the other domains within its own module: 1) the AT, which loads the extender unit, 2) the KS, which catalyzes chain extension, and 3) all of the reductive domains that process the resulting β-ketone. In addition, the ACP transfers the fully processed intermediate either to a downstream KS in the next module, or to the TE. The molecular details of these interactions—the spatial relationships among the domains as well as the nature,

[a] *L. Tran, Prof. P. F. Leadlay, Dr. K. J. Weissman*
Department of Biochemistry, University of Cambridge
80 Tennis Court Road, Cambridge CB2 1GA (UK)

[b] *Dr. M. Tosin, Dr. J. B. Spencer*
Department of Chemistry, University of Cambridge
Lensfield Road, Cambridge CB2 1EW (UK)

[c] *Dr. K. J. Weissman*
Present address:
Department of Pharmaceutical Biotechnology, Saarland University
P.O. Box 151150, 66041 Saarbrücken (Germany)
Fax: (+49)681-302-5473
E-mail: k.weissman@mx.uni-saarland.de

Supporting information for this article is available on the WWW under http://www.chembiochem.org or from the author.

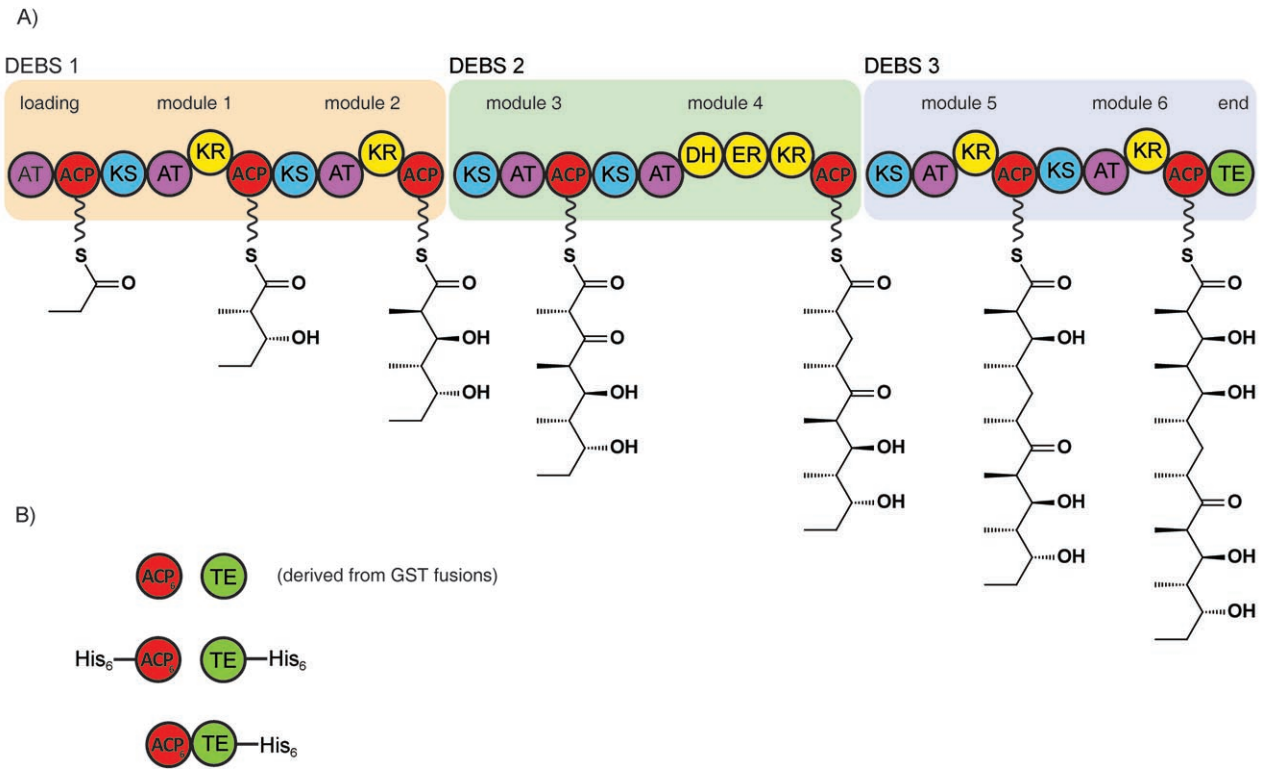

Figure 1. A) The erythromycin PKS (6-deoxyerythronolide B synthase, DEBS) consists of a loading module, six chain-extension modules, and a chain-terminating thioesterase (TE), distributed across three giant polypeptide chains named DEBS 1, 2, and 3. Each chain-elongation module contains an acyl transferase (AT), a ketosynthase (KS), and an acyl carrier protein (ACP) domain, and an optional combination of reductive domains (DH, dehydratase; ER, enoyl reductase; KR, ketoreductase). B) Graphical representation of protein constructs used in this study. His_6 indicates the presence of a hexameric histidine tag.

strength, and dynamics of their interfaces—are key to a deeper understanding of the biosynthetic process. The basis for ACP communication is also of particular interest for future genetic engineering efforts, as the ability to obtain functional hybrid synthases by substituting individual domains or modules depends critically on deciphering how interdomain interactions are coordinated and regulated.

In type II FAS and PKS systems in which domains are present as individual components, interactions between the proteins must occur through compatible molecular interfaces. A variety of structural and mutational studies have identified helix αII of FAS ACPs as a universal recognition element,[14–17] and modeling of the interface between type II PKS ACP and KR domains has also implicated this helix.[18] Swapping of ACP domains between different type II PKS or FAS systems often leads to partial or complete loss of function, which might be explained, at least in part, by the existence of highly specific recognition motifs on these domains.[19–21] In comparison with other regions of the proteins, helix αII is more highly conserved among known ACPs, including those from type I PKSs.[22] Recent experiments have shown that residues in helix αII of ACP_6 from the erythromycin-producing PKS (DEBS) mediate its interactions with phosphopantetheinyl transferases (PPTases),[23] the enzymes responsible for converting ACPs from their *apo* to *holo* forms by attachment of Ppant.[24] Furthermore, computational docking and site-directed mutagenesis of DEBS ACPs support the role of helix αII and the adjacent loop region in recognition between ACP and KS domains.[13,25] Together, these data suggest that type I ACP domains may use structural features similar to those present on type II ACPs to interact with partner enzymes. However, it is also possible that the structural arrangement and covalent linkage of ACPs to other domains within type I PKSs suffice to ensure productive contacts.

To gain further insight into ACP-based communication, we have explored in detail the interaction between DEBS ACP_6 and the downstream TE domain to which it is directly joined within the multienzyme through a linker of eleven amino acid residues.[26,27] Our analysis both by surface plasmon resonance and isothermal titration calorimetry confirmed that the separate proteins do interact, albeit with relatively modest affinity, and that the association is enhanced by the presence of the Ppant arm and the acyl chain. However, we also show that the TE is dramatically less effective at hydrolyzing a butyryl group (a model of the polyketide acyl group) from a discrete ACP_6 than from an ACP_6 domain to which it is covalently tethered.[28] Taken together, our results suggest that a major determinant of the efficiency of TE catalysis of acyl chain transfer from the ACP is the covalent linkage of the two domains into a single polypeptide, with only a minor contribution from recognition of a specific interface or of the phosphopantetheine-bound moiety. Thus, despite the obvious mechanistic similarities be-

tween type I and type II PKS systems, there appear to be significant differences in key protein–protein interactions within these multienzymes. If other ACP-based interactions within each PKS module turn out to be similarly governed by covalency and proximity, it should significantly advance genetic engineering of these systems.

Results

Design of the experimental system

To evaluate the contribution of covalent linkage to interdomain interactions, we elected to compare the ACP_6-TE didomain of the erythromycin-producing PKS (DEBS)[28] with the ACP_6 and TE components expressed as discrete proteins. Previous studies have established that the ACP_6 domain of ACP_6-TE can be quantitatively phosphopantetheinylated in vitro,[23] and that the TE can hydrolyze a wide range of model substrates derivatized as their nitrophenyl esters.[29,30] ACP_6 was successfully expressed as a C-terminal translational fusion with GST, from which it was released by cleavage with PreScission Protease, and with an N-terminal His_6 tag (Figure 1). Domain boundaries were selected on the basis of literature precedent.[31] We confirmed the structural integrity of each ACP species by treatment with the broad-specificity phosphopantetheinyl transferase Sfp,[32] followed by analysis by high-pressure liquid chromatography–mass spectrometry (HPLC-MS). Modification by phosphopantetheine was quantitative, and the ACP_6 could be produced fully acylated with the polyketide mimic butyrate by incubation with butyryl-CoA and Sfp (Figure 2). Butyryl-ACP_6 was found to be stable under the acidic conditions required to quench TE-catalyzed hydrolysis, which permitted kinetic analysis of the rate of chain release from ACP_6.

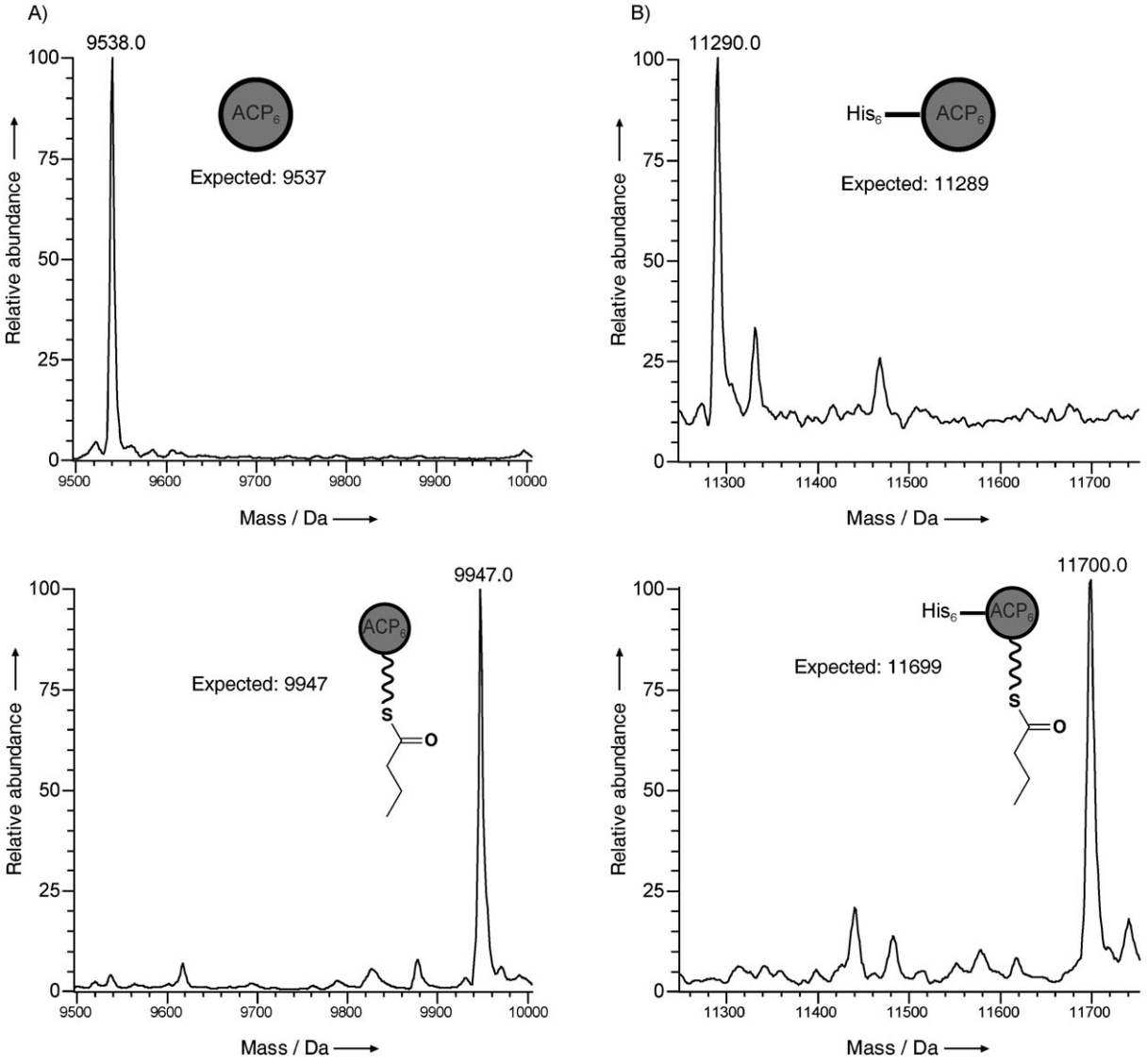

Figure 2. HPLC-MS traces showing acylation of ACP_6 constructs with butyrate after 1 h incubation with Sfp and butyryl-CoA. A) Acylation of untagged ACP_6. B) Acylation of N-terminally His_6-tagged ACP_6.

The recombinant TE domain was designed to include all of the ACP_6-TE linker region, a construct closely similar to that used previously to study TE domain specificity.[33] The TE was obtained both as a GST fusion protein and with a C-terminal His_6 tag. Although the DEBS TE normally accomplishes chain release by macrolactonization with the aid of a distal hydroxyl nucleophile on the polyketide intermediate, alternative hydrolytic release of model substrates is also efficient.[29,30] We therefore chose to evaluate the catalytic activity of the TE by using a commercially available nitrophenolate ester. Both forms of the TE were found to catalyze hydrolysis of *p*-nitrophenylbutyrate with a k_{cat} of $8.3 \pm 0.2\ s^{-1}$, comparable to that of the ACP-TE didomain ($8.1 \pm 0.3\ s^{-1}$), demonstrating that the discrete TEs were properly folded and catalytically competent (Figure 3).

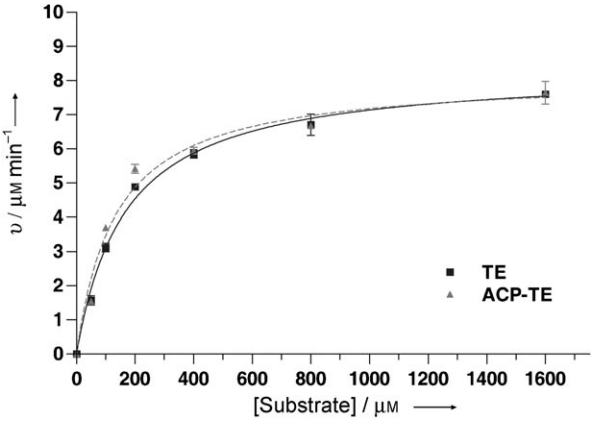

Figure 3. Hydrolysis of the model substrate *p*-nitrophenyl butyrate by recombinant TE and ACP_6-TE. The data were fit to the Michaelis–Menten equation by nonlinear regression.

Hydrolysis of butyryl-ACP by covalently tethered TE is rapid

We next attempted to quantify the rate of release of butyrate from butyryl-ACP_6 housed within the ACP_6-TE didomain. The ACP_6-TE (3 μM) was incubated with butyryl-CoA and Sfp (300 pM) for various periods, followed by quenching with glacial acetic acid and analysis by HPLC-MS. This experiment provided no evidence of a butyryl moiety on either the ACP_6 or the TE domains. Although the majority of the ACP_6 protein was in its phosphopantetheinylated *holo* form, a small proportion of the domain was *apo* even after 1 h incubation, suggesting that transfer of the butyryl-pantetheine group to ACP_6 was slow under the assay conditions (Figure 4). We therefore repeated the experiments with a 100-fold higher concentration of Sfp (30 nM), so that transfer of the butyrate substrate to ACP_6 was not expected to be rate-limiting. Again, however, at all time points tested (1–60 min), the major peak in the HPLC-MS chromatogram corresponded to *holo*-ACP, with no evidence of butyryl groups on either the ACP or TE domains (Figure 4). This result suggested that transfer of the butyryl-phosphopantetheine moiety to ACP_6, transesterification to the TE, and TE-catalyzed hydrolysis all occurred within the "dead time" of the experiment—that is, as soon as the butyryl group was present on the ACP, it was transferred to and hydrolyzed by the TE domain.

In principle, it was possible that the Sfp had preferentially utilized a minor CoA contaminant in the commercial sample of butyryl-CoA during the phosphopantetheinylation reaction, thus generating *holo*-ACP directly. To rule out this possibility, we constructed an active site Ser to Ala mutant in the TE (TE_{S3029A}; numbered as for DEBS 3) to disable both its acyl transfer and hydrolytic activities (this mutation had previously been shown not to disrupt the overall folding of the upstream ACP[34]). Incubation of the mutant ACP_6-TE didomain with butyryl-CoA and Sfp, followed by HPLC-MS analysis, showed that butyryl-ACP_6 was formed quantitatively and stably (Figure 4). The finding that *holo*-ACP_6 was observed at all time points with the ACP_6-TE wild-type didomain therefore suggests that initial formation of butyryl-ACP_6 is followed by immediate TE-catalyzed release.

Hydrolysis of butyryl-ACP by discrete TE is inefficient

We next examined hydrolysis of butyryl-ACP_6 by discrete TE-His_6 (Figure 5). As controls, we analyzed the concentration dependence of the initial rate of hydrolysis by a fixed amount of TE of the butyryl-ACP_6 mimics butyryl-CoA and butyryl-pantetheine (see the Experimental Section). These reactions were carried out in the presence of Ellman's reagent—5,5′-dithiobis-(2-nitrobenzoic acid) (DTNB)—and the rate of release of free thiol was measured by UV-visible spectroscopy.[35] Only low rates of hydrolysis were observed for these simple thioesters, at all concentrations tested (Figure 5B).

Butyryl-ACP_6 (1 μM) was generated as described above and incubated with increasing amounts of discrete TE (1, 3.1, 10, 31, and 100 equivalents). Analysis of the ACP_6 at various time points by HPLC-MS showed that release of butyrate was dramatically slowed in relation to the very rapid hydrolysis by the ACP_6-TE didomain (compare Figures 5A and C with Figure 4). The effect of removing the tether is expressed in a greatly decreased k_{cat} ($0.046 \pm 0.002\ s^{-1}$), rather than in greatly weakened binding (the apparent K_M of treating the TE as the "substrate" was 1.2 ± 0.2 μM (Figure 5A)).

Direct analysis of ACP binding to TE by SPR

Surface plasmon resonance (SPR) was used to assess binding of the TE to various forms of ACP_6 (*apo*, *holo*, and butyryl). Initial attempts to couple untagged ACP_6 to the SPR chip by standard amine chemistry were successful, but no binding was detected either to discrete TE-His_6 domain, or to Sfp as a positive control. Unfortunately, direct immobilization often decreases or completely abrogates binding to analytes in SPR,[36] because the binding surface is occluded by the immobilization. In the case of ACP_6, sequence analysis suggests that coupling should have occurred exclusively through the N-terminal Gly residue. As an alternative, we immobilized His_6-tagged ACP_6 on a Ni-NTA chip. Although no signal was observed when the TE was applied to bound *apo*-ACP_6, an interaction was detected between the TE and both *holo*- and butyryl-ACP_6 (Figure 6).

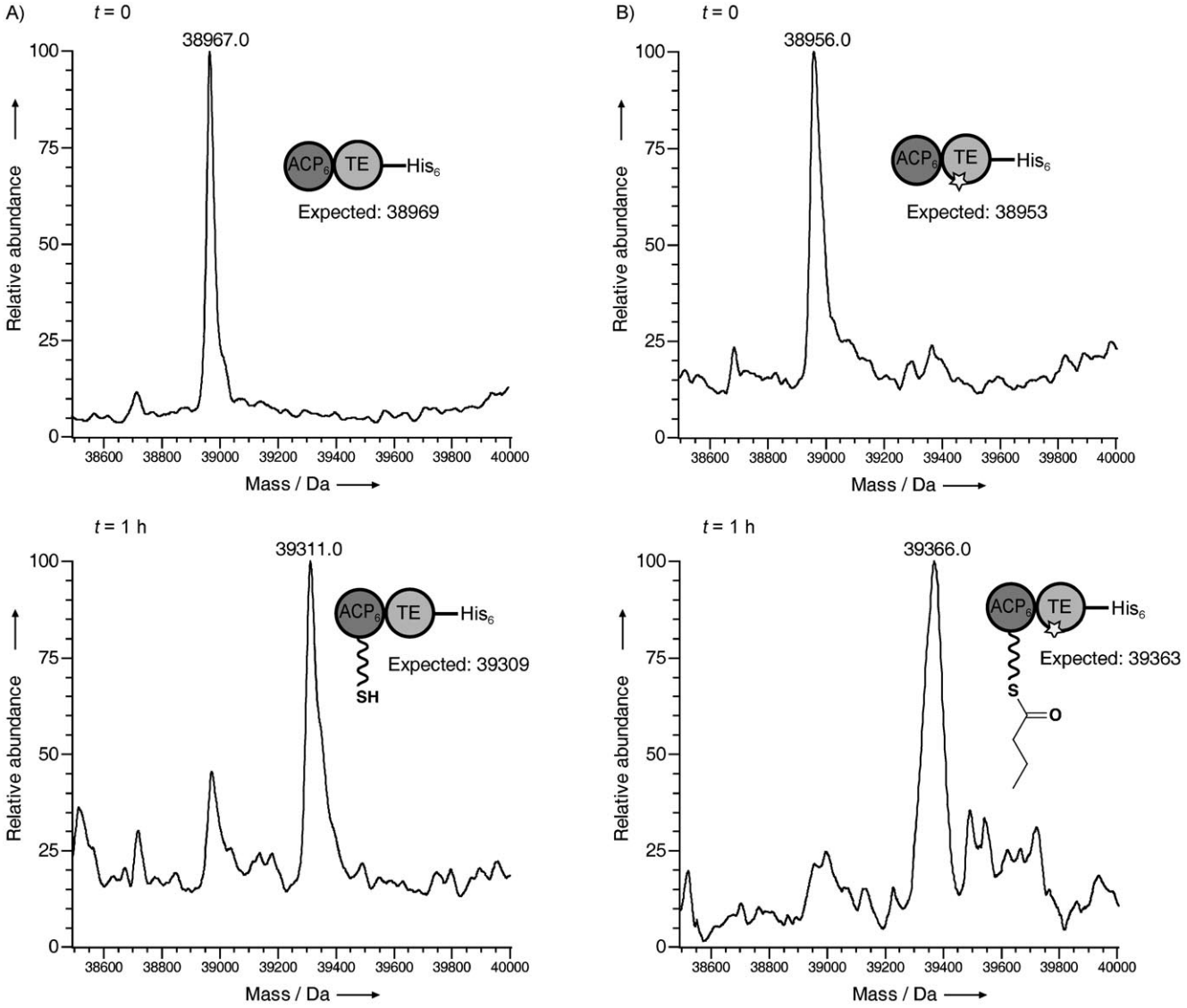

Figure 4. HPLC-MS traces showing incubation of ACP_6-TE constructs with Sfp and butyryl-CoA. A) Wild-type ACP_6-TE. B) ACP_6-TE containing active site S3049A mutation.

Flowing Sfp over *apo*-ACP_6 also resulted in a significant signal (Figure 6).

Although the sensorgrams revealed a clear trend of increasing binding affinity (*apo* ≪ *holo* < butyryl), attempts to fit the data to a simple one-site binding model (Langmuir isotherm) were not successful. It is possible that the chip surface contained a heterogeneous population of ACP_6 domains,[36] even though immobilization through the His_6 tag ought to have yielded a single orientation of ACP_6 on the chip. There was certainly a low, but consistent, level of non-specific binding between untagged ACP_6 and the Ni-NTA surface, probably due to the acidic character of the ACP_6 domain (pI 5.3). This non-specific binding also frustrated attempts to analyze the interdomain interaction by flowing ACP_6 over the TE bound to the chip through its His_6 tag. We also immobilized His_6-tagged TE by using an anti-His_6 antibody. However, the TE domain attached in this way did not interact with ACP_6 to any measurable extent (data not shown). Putative recognition sites for the ACP_6 have been proposed to lie close to the subunit interface on the TE,[27] and this arrangement might be sensitive to perturbation caused by immobilization.

Direct analysis of ACP binding to TE by ITC

As an alternative to SPR, isothermal titration calorimetry (ITC) was used to measure the binding affinity. The major advantage of this technique is that binding is assessed between native, unmodified proteins in solution, removing the requirement to immobilize either partner.[37] The mutant TE_{S3029A} (100 μM) was titrated at 20 °C with either *apo*-, *holo*-, or butyryl-ACP_6 (all at 2 mM; Figure 7). This analysis revealed the same trend in binding affinity as had been seen with SPR. Titration with the *apo* protein did not produce any detectable signal. The *holo* protein did show detectable binding, although the heat signal

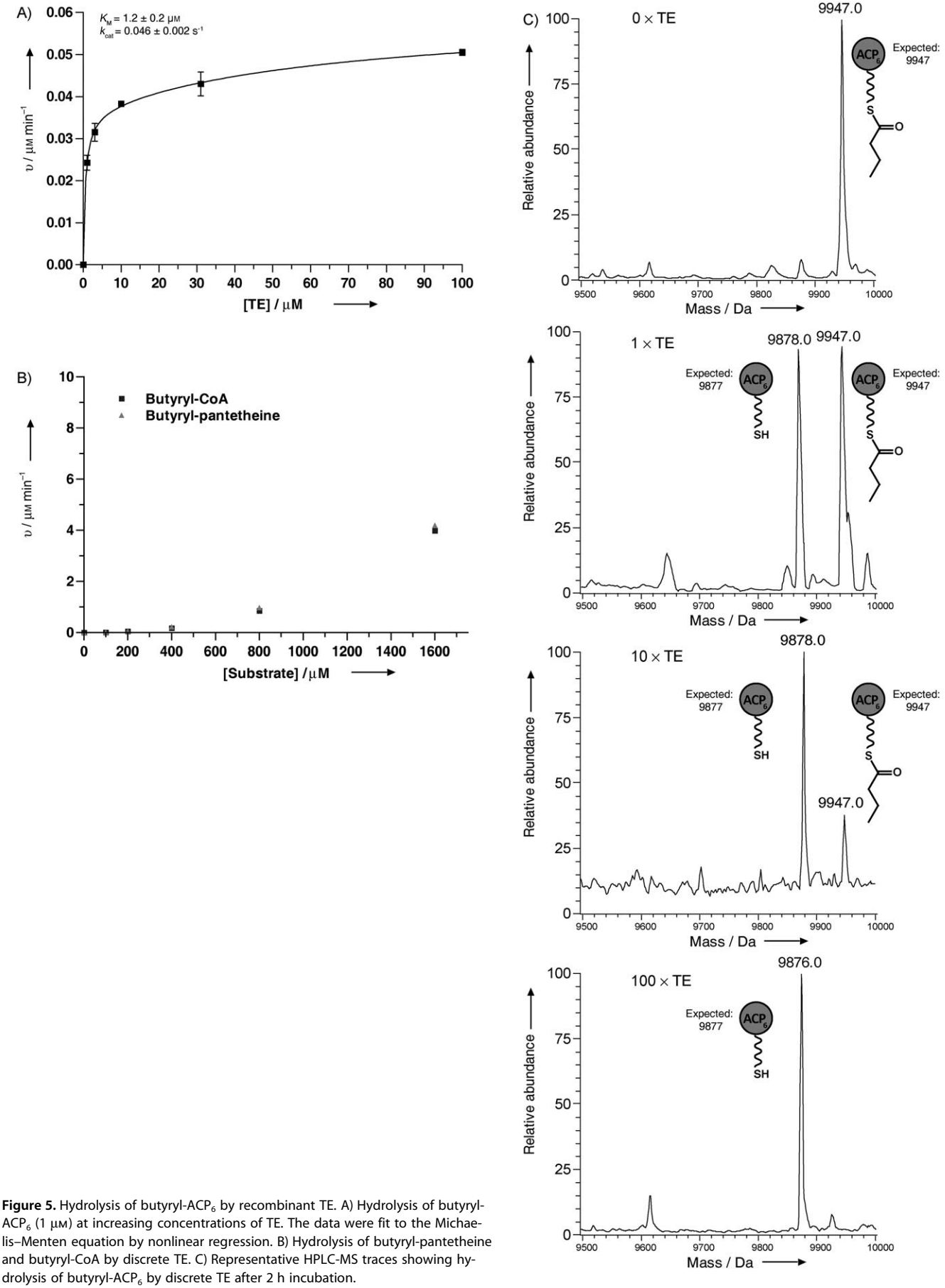

Figure 5. Hydrolysis of butyryl-ACP$_6$ by recombinant TE. A) Hydrolysis of butyryl-ACP$_6$ (1 μM) at increasing concentrations of TE. The data were fit to the Michaelis–Menten equation by nonlinear regression. B) Hydrolysis of butyryl-pantetheine and butyryl-CoA by discrete TE. C) Representative HPLC-MS traces showing hydrolysis of butyryl-ACP$_6$ by discrete TE after 2 h incubation.

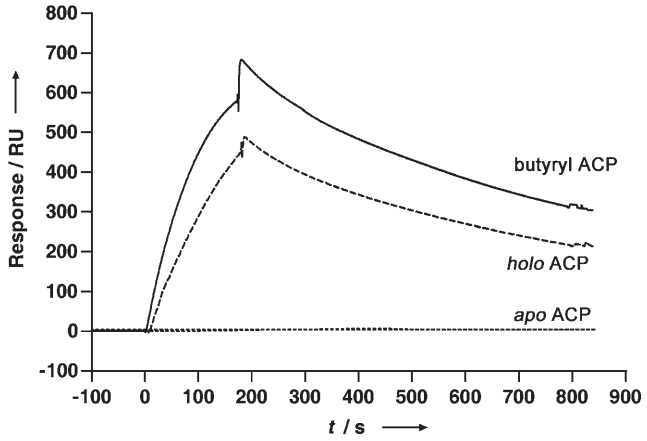

Figure 6. SPR analysis of the interaction between ACP_6 and TE. Sensorgrams of the interaction of TE with *apo*, *holo*, and butyryl forms of ACP_6 at 400 μM are shown.

was insufficient for a reliable K_D to be calculated. For butyryl-ACP_6, the data could be convincingly fit to a one-site binding model, yielding a K_D value of 18 ± 1 μM (Figure 7).

Discussion

Comparison of type II and modular type I PKSs, which catalyze a closely similar set of reactions, suggests that at least some domains within PKSs interact through specific recognition surfaces. Indeed, subtle changes in the natures of these interfaces during catalysis might form the basis for specific programming, in which each module catalyzes a single cycle of chain extension before handing on the polyketide chain to the neighboring downstream module. Further, failure to maintain the integrity of such interprotein interfaces in engineered PKSs may account for the observed inefficiency[1] or inactivity[38,39] of these hybrids. This remains an appealing mechanism. Our results suggest, however, that an additional and indispensable contribution to efficient communication between the ACP and TE domains is their covalent tethering through a linker.[40] The lack of sequence conservation in this interdomain region among modular PKSs (see the Supporting Information), the shorter length of the sequence (10–45 residues) in relation to other linkers that adopt folded structures (for example, KS-AT (100 residues);[41] AT-KR (280 residues)[40,42] in a typical PKS), and an amino acid composition rich in Pro, Ala, and charged residues[43] are all consistent with the idea that this region serves as a flexible tether that promotes the close approach of the two domains. This region of the DEBS subunit is also susceptible to limited proteolytic cleavage[44]—further evidence that it is unstructured in its native context. Such properties have been demonstrated for the analogous linker region bridging the ACP and TE activities of animal FASs.[45] Indeed, it has further been shown that a FAS TE domain released from the upstream ACP by limited proteolysis retained activity with acyl-CoA substrate but not with the remainder of the multienzyme,[46] consistent with the lack of a strong protein–protein interaction in the absence of a tether between the ACP and TE domains.[47] Covalent tethering is also likely to position the substrate optimally relative to the TE active site; indeed, our kinetic data suggest that nonproductive binding modes are favored in the absence of the linker region.

Nevertheless, the kinetic data for hydrolysis of butyryl-ACP_6 by the TE (Figure 5) indicate a contribution from molecular recognition. To localize the region on ACP_6 that is involved in binding the TE, we evaluated the interaction between the TE and either *apo*-, *holo*-, or butyryl-ACP_6 by both ITC and SPR. Neither approach (Figures 6 and 7) provided any evidence for binding between the TE and the *apo*-ACP. An interaction was observed between the TE and the *holo* protein, and the affinity of binding was increased further by the presence of a butyryl

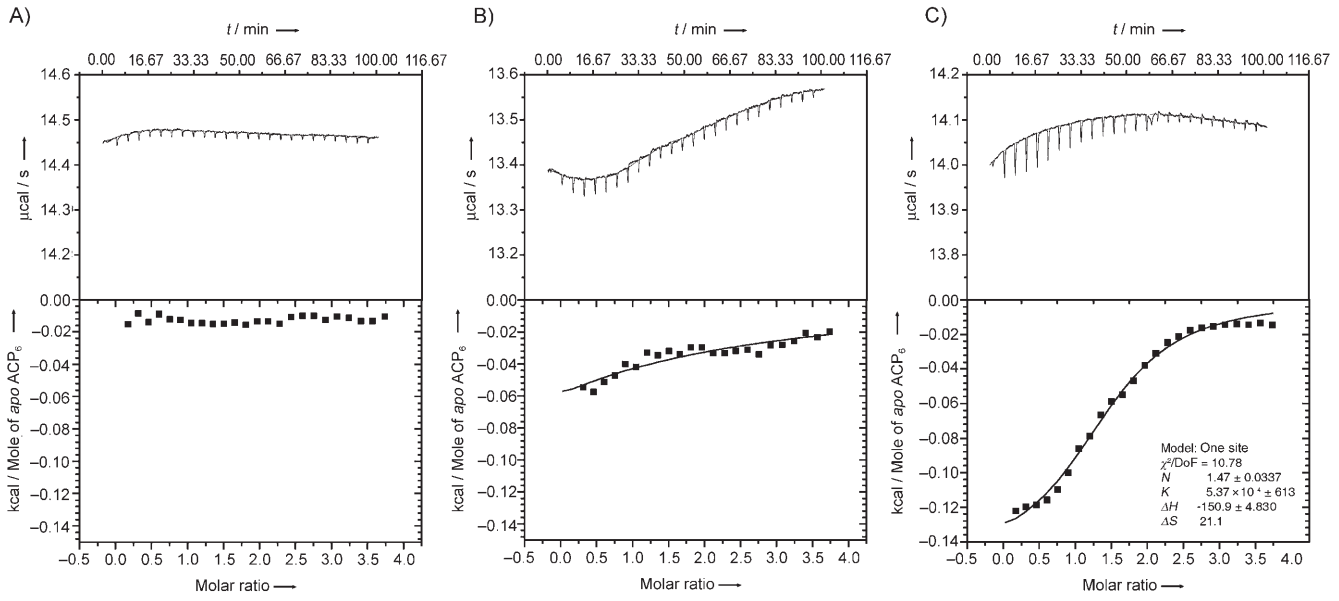

Figure 7. Representative ITC analysis of TE_{S3029A} (100 μM) titrated with A) *apo*-ACP_6, B) *holo*-ACP_6, and C) butyryl-ACP_6 (all at 2 mM).

chain. Taken together, these data suggest that the most significant interaction occurs between the TE and the prosthetic group (as well as the attached acyl moiety), and not with the ACP itself. Surprisingly, we did not observe a significant rate of hydrolysis of the model substrates butyryl-CoA or pantetheinyl butyrate by the TE, even at high substrate concentrations. However, pantetheine lacks the terminal phosphate of Ppant, while CoA incorporates an additional AMP moiety, making the compounds only imperfect mimics of the Ppant arm. Thus, one plausible interpretation of this result is that the single phosphate group of Ppant makes a significant contribution to substrate recognition by the TE. An alternative explanation is that the Ppant interacts with the ACP domain, adopting a specific conformation that enhances its binding to the TE. However, for the majority of ACP domains characterized to date, contacts have not been observed between the protein and the prosthetic arm.[8,9,48,49] These data also argue against the possibility that phosphopantetheinylation and/or acylation induce changes in the ACP structure that result in tighter binding to the TE. Indeed, no evidence that ACP_2 of DEBS exhibits conformational heterogeneity in solution was reported.[13] Together, these results suggest that the increase in affinity observed in the SPR and ITC experiments was due to recognition by the TE of the groups tethered to the ACP domain, although further data will be required to rule out the alternative explanations conclusively.

The fact that the interaction between the ACP and the TE is substantially governed by proximity accounts, at least in part, for the empirical observation that TE domains can effect efficient chain release from multiple non-cognate ACP domains in engineered systems.[34,50,51] Thus, the primary determinant of its function would seem to be specificity for the substrate acyl group attached to the ACP and the presence of a suitably positioned nucleophile with which to accomplish lactonization or hydrolysis.[52,53] Similar conclusions supporting the role of proximity have recently been reached for recombinant PKS KR domains, which showed specificity for their β-ketoacylthioester substrates, but not for the ACP domains to which the substrates were tethered, nor for the KS domains that synthesized the intermediates.[54] The primacy of covalent linkage in governing the interaction between the DEBS TE domain and the ACP is encouraging for future genetic engineering efforts, because it suggests that as long as the proper architectural relationship is maintained and the substrate contains appropriate recognition features for the TE, then efficient chain transfer and release will occur.

Experimental Section

Cloning procedures: The following constructs were amplified by PCR from pACP-TEHis:[23] untagged ACP_6 (primers; 5′-TGT-TGG ATC CGC GGC CCC GGC GCG GGA GAT GAC GTC GCA GGA GTT-GCT GG-3′ [forward] and 5′-GAG TC GAA TTC TCG AGC TGC TGT CCT-ATG TGG TCG-3′ [reverse]); His-ACP_6 (primers; 5′-GAA ATA ATT TTG-TTC ATA TGG CGG CCC CGG CGC GGG AGA TGA CGT CGC AGG AGT TGC-3′ [f] and 5′-GAG TC GAA TTC TCG AGC TGC TGT CCT ATG TGG TCG-3′ [r]); and TE (primers; 5′-GAT ATA GGA TCC GAC AGC GGG ACT CC-3′ [f] and 5′-CGA GGA ATT CTT AGC TAT TCC CTC CGC CC-3′ [r]). Untagged ACP_6 and TE were subsequently cloned into pGEX-6P-1 previously digested with BamHI and EcoRI. His-ACP_6 was cloned into pET28b+ previously digested with NdeI and EcoRI. pKJW63 (TE-His_6) was constructed by amplification of the linker-TE region from pIB023 (primers; 5′-AAT TCA TAT GGA CAG CGG GAC TCC CGC CCG G-GA A-3′ [f] and 5′-TTG CGG CCG CTG GAA TTC CCT CCG CCC A-3′). The resulting PCR product was subcloned into pUC18, before digestion and subsequent cloning into pET29b+ previously digested with NdeI and NotI.

Site-directed mutagenesis of ACP_6-TE: Plasmid pACP-TEHis[23] was mutated by QuickChange mutagenesis (Stratagene) according to the manufacturer's instructions with use of the mutagenic primers, 5′-GGT GGC CGG TCA C**G**C CGC GGG GGC AC-3′ (sense) and 5′-GTG-CCC CCG CGG **C**GT GAC CGG CCA CC-3′ (antisense), encoding for the active site S3029A mutation (the modified sequence is underlined). The mutant plasmids were then sequenced between naturally occurring SacI and DraIII sites within the ACP_6-TE gene, and the correct sequences were then excised as SacI-DraIII fragments and cloned into unmutated pACP$_6$-TEHis previously digested with both SacI and DraIII.

Expression and purification of untagged constructs from their GST fusion proteins: Expression constructs (ACP_6, TE) were transformed into *E. coli* BL21 (DE3) CodonPlus-RP cells. Cultures were grown in LB medium (2 L) supplemented with carbenicillin (100 μg mL^{-1}) and chloramphenicol (34 μg mL^{-1}) to an OD_{600} of 0.8, and induced with isopropyl-β-D-thiogalactopyranoside (IPTG; 0.2 mM); expression was carried out overnight at 22 °C or 37 °C. Following expression, cells were harvested by centrifugation and frozen at −20 °C. Cell pellets were resuspended in Tris-Triton X buffered saline (TTBS; 20 mM Tris-HCl (pH 7.4), 150 mM NaCl, 0.1% Triton-X), supplemented with protease inhibitor cocktail (Roche), benzonase (Novagen, 8 U), and ready-lyse lysozyme (Epicentre Biotechnologies, 250 kU), and left to incubate on ice for 30 min. Cells were ruptured by sonication (Misonix, Inc.), and the protein supernatant was isolated by centrifugation at 21 000 *g* for 30 min. The cell lysate was then applied to a glutathione agarose column. The column was washed with 5 column volumes of TTBS and 5 column volumes of TBS (20 mM Tris-HCl (pH 7.4), 150 mM NaCl) before equilibration in PreScission Protease cleavage buffer (50 mM Tris-HCl (pH 8.0), 100 mM NaCl, 1 mM EDTA, 1 mM DTT). On-column cleavage was performed with PreScission Protease (GE Healthcare, 100 U) in 1 column volume of cleavage buffer, at 4 °C overnight. The target fusion partner was eluted in cleavage buffer and then concentrated and exchanged into PBS (50 mM NaPi (pH 7.0), 150 mM NaCl) with a PD-10 column.

Expression of His_6-tagged proteins: Expression constructs (His_6-ACP, ACP-TE-His_6, TE-His_6) were transformed into *E. coli* BL21 (DE3) CodonPlus-RP cells. Cultures were grown in LB medium (2 L) supplemented with kanamycin (50 μg mL^{-1}) and chloramphenicol (34 μg mL^{-1}) to an OD_{600} of 0.8, and induced with IPTG (1.0 mM); expression was carried out overnight at 22 °C or 37 °C. Following expression, cells were harvested by centrifugation and frozen at −20 °C. Cell pellets were resuspended in chilled Ni-NTA buffer (50 mM sodium phosphate buffer (pH 8.0), 300 mM NaCl, 0.1% Triton-X), supplemented with protease inhibitor cocktail, benzonase (8 U), and ready-lyse lysozyme (250 kU), and left to incubate on ice for 30 min. Cells were ruptured by sonication, and the protein supernatant was isolated by centrifugation at 21 000 *g* for 30 min. Cell lysate was incubated with Ni-NTA resin (Sigma, 5 mL) for 1 h at 4 °C. The resin was then transferred to a column, and washed with 10 column volumes of Ni-NTA buffer containing

imidazole (20 mM). His-tagged protein was eluted with imidazole (250 mM) in Ni-NTA buffer (pH 7.0). Imidazole was removed by buffer exchange on a PD-10 desalting column into PBS (50 mM sodium phosphate buffer (pH 8.0), 150 mM NaCl).

Phosphopantetheinylation and acylation of ACP_6: Untagged ACP_6 (3 μM) was incubated with Sfp (31 nM), in buffer (50 mM NaPi (pH 6), 10 mM $MgCl_2$, 5 mM DTT, 1 mM CoASH (or acyl-CoASH)) in a 100 μL reaction volume.[22] Reactions were allowed to proceed at 37 °C for 1 h, before quenching with glacial acetic acid (1 μL) and snap freezing in liquid nitrogen. Samples were subsequently stored at −80 °C until analysis by HPLC-MS. Analysis was performed on a HP 1100 (Hewlett–Packard, Wilmington, DE, USA) high-pressure liquid chromatography system coupled with an LCQ Classic (ThermoFinnigan, San Jose, USA) mass spectrometer fit with an electrospray ionization source. Samples were applied to a reverse phase column (Vydac, Protein C4, 5 μm, 250×4.6 mm, 300 Å) and eluted with a linear gradient from 25–95% acetonitrile/water containing trifluoroacetic acid (0.1%), over 20 min at a flow rate of 1 mL min^{-1}. The eluent was monitored by use of a diode array detector at 214 and 280 nm. The mass spectrometer was set to a spray voltage of 4.5 kV and a capillary temperature of 200 °C. The HPLC-MS system was controlled with Xcalibur (version 1.1, ThermoFinnigan, San Jose, CA, USA), and mass spectrometric data were processed and transformed by use of Bioworks software (version 1.1, ThermoFinnigan).

Assays for thioesterase activity: Purified TE-His and ACP_6-TE-His_6 (1.31 μM) were incubated with varying concentrations of *p*-nitrophenyl butyrate (Sigma) in buffer (200 mM NaPi, 2.5 mM Tris buffer (pH 7.0), 50 μM EDTA, 5 μM DTT).[29] Reactions in duplicate were performed at 30 °C and monitored with a UV spectrophotometer (Shimadzu) at 400 nm. Reactions were measured against the background rates of hydrolysis in the absence of the proteins.

Synthesis of butyryl pantetheine: D-Pantethine (276 mg, 0.498 mmol) was dissolved in dry isopropanol (5 mL) under argon; the solution was degassed by bubbling in argon for 40 min. Sodium borohydride (92 mg, 2.432 mmol) was added, and the mixture was heated to reflux (85 °C) for 16 h. Once the reaction was judged complete by TLC analysis, the mixture was allowed to cool to room temperature and diluted with methanol (10 mL); acetic acid (2.8 mL) was then added to destroy the excess hydride, and the mixture was concentrated in vacuo. The crude product, a transparent oily liquid, was carried on to the next step without purification. Analytical data for D-pantetheine: R_f: 0.55 (ethyl acetate/methanol 3:1), ^{1}H NMR (400 MHz, D_2O): $\delta = 3.90$ (s, 1H; CH), 3.44 (t, $^3J_{H,H} = 6.0$ Hz, 2H; CH_2), 3.43 (d, $^3J_{H,H} = 11.0$ Hz, 1H; $CH_{2a}OH$), 3.31 (d, $^3J_{H,H} = 11.0$ Hz, 1H; $CH_{2b}OH$), 3.29 (t, $^3J_{H,H} = 6.5$ Hz, 2H; CH_2), 2.57 (t, $^3J_{H,H} = 6.5$ Hz, 2H; CH_2), 2.44 (t, $^3J_{H,H} = 6.0$ Hz, 2H; CH_2), 0.84, 0.81 ppm (s, 3H; $C(CH_3)_2$); ^{13}C NMR (100 MHz, D_2O): $\delta = 174.1$, 173.0 (CONH), 74.8 (CH), 67.3 (CH_2OH), 41.2 (CH_2), 37.6 ($C(CH_3)_2$), 34.4, 34.3, 22.1 (CH_2), 19.4, 18.1 ppm ($C(CH_3)_2$); ESI-MS: 578.8 $[2M+Na]^+$, 301.1 $[M+Na]^+$, 278.8 $[M+H]^+$, 261.2 $[(M-H_2O)+H]^+$.

D-Pantetheine was directly dissolved in dry THF (7 mL) at 0 °C in the presence of triethylamine (0.42 mL, 3.013 mmol); butyryl chloride (0.10 mL, 0.963 mmol) was added dropwise. The reaction was stirred at 0 °C for 1 h and at room temperature for a further 3 h, after which the solvent was removed under reduced pressure. Water and ethyl acetate (10 mL of each) were then added to the crude residue; the organic phase was isolated, dried over $MgSO_4$, filtered, and concentrated to afford the final product as a clear oil (213 mg, 61% over two steps). For enzymatic assays, a small amount of this material was further purified by semipreparative HPLC (Polar RP 80 A-column, 250×10.00 mm, 4 μm, 2.5 mL min^{-1}, from 100% water to 100% acetonitrile in 30 min, $t_R = 17.5$ min). Analytical data for D-butyryl-pantetheine: ^{1}H NMR (400 MHz, D_2O): $\delta =$ 3.91 (s, 1H; CH), 3.43 (d, $^3J_{H,H} = 11.0$ Hz, 1H; $CH_{2a}OH$), 3.41 (t, $^3J_{H,H} =$ 7.0 Hz, 2H; CH_2), 3.32 (d, $^3J_{H,H} = 11.0$ Hz, 1H; $CH_{2b}OH$), 3.30 (t, $^3J_{H,H} =$ 6.5 Hz, 2H; CH_2), 2.97 (t, $^3J_{H,H} = 6.5$ Hz, 2H; CH_2), 2.55 (t, $^3J_{H,H} =$ 7.5 Hz, 2H; CH_2), 2.39 (t, $^3J_{H,H} = 7.0$ Hz, 2H; CH_2), 1.58 (sextet, $^3J_{H,H} =$ 7.5 Hz, 2H; CH_2), 0.84 (t, $^3J_{H,H} = 7.5$ Hz, 3H; CH_2CH_3), 0.84, 0.81 ppm (s, 3H, $C(CH_3)_2$); ^{13}C NMR (100 MHz, D_2O): $\delta = 204.4$ (SCO), 174.7, 173.6 (CONH), 75.4 (CHOH), 68.0 (CH_2OH), 45.0, 38.3 (CH_2), 38.2 ($C(CH_3)_2$), 35.0, 34.9, 27.6 (CH_2), 20.1, 18.7 ($C(CH_3)_2$), 18.6 (CH_2), 12.2 ppm (CH_2CH_3); HR-ESMS: found 349.1786; required: 349.1797 $[M+H]^+$.

Assay for hydrolysis of butyryl-pantetheine and butyryl-CoA: Varying concentrations of substrate were incubated with the TE-His_6 (1 μM) in buffer (50 mM NaPi buffer (pH 7.4), 150 mM NaCl, 0.2 mM 5, 5′-dithiobis-(2-nitrobenzoic acid) (DTNB)). Free thiol groups were then detected by reaction with DTNB, with monitoring at 412 nm using a UV/Vis spectrophotometer (Shimadzu). Reactions were measured against the background rates of hydrolysis in the absence of the TE.

Detection of hydrolysis of butyryl-ACP_6 and butyryl-ACP_6-TE by HPLC-MS: Preformed untagged butyryl-ACP_6 (1 μM) and TE-His (varying) were incubated at 37 °C for the indicated periods in buffer (50 mM NaPi buffer (pH 7.4), 150 mM NaCl) (Figure 5). The reactions were quenched with glacial acetic acid (1 μL), and the products were analyzed by HPLC-MS, as described previously. ACP_6-TE-His_6 (1 μM) was incubated at 37 °C with Sfp (31 nM) in buffer (50 mM NaPi (pH 6), 10 mM $MgCl_2$, 5 mM DTT) containing butyryl-CoASH (1 mM) for 1, 5, 15, 30, and 60 min. The reactions were quenched with glacial acetic acid (1 μL), and the products were analyzed by HPLC-MS. For the hydrolysis of butyryl-ACP_6, data obtained from two independent determinations were fit to the Michaelis–Menten equation by nonlinear regression (SigmaPlot).

Surface plasmon resonance (SPR): SPR experiments were performed on a Biacore 2000 instrument (Biacore AB).

Direct immobilization of ACP_6 was performed with a CM5 chip (Biacore AB). The chip was activated by injection of freshly prepared *N*-ethyl-*N*′-(3-dimethylaminopropyl)carbodiimide (EDC; 0.2 M) and *N*-hydroxysuccinimide (NHS, 0.05 M; 1:1, 200 μL) at a flow rate of 5 μL min^{-1} at 25 °C. ACP_6 was coupled to the chip by injection of protein (500 μg mL^{-1}) in running buffer (10 mM HEPES-KOH buffer (pH 7.4), 150 mM NaCl, 3 mM EDTA, 0.005% P20 surfactant) for 3 min, followed by ethanolamine (1.0 M, 100 μL) to deactivate any remaining active ester sites. ACP_6 (800 response units (RUs)) was immobilized on the CM5 surface. Binding experiments were conducted by injection of TE at different concentrations in running buffer (10 mM HEPES (pH 7.4), 150 mM NaCl, 50 μM EDTA, 10 mM imidazole and 0.005% P20 surfactant) at a flow rate of 10 μL min^{-1} for 3 min. As a control, Sfp (10 μM) was flowed over ACP_6 immobilized to the CM5 surface, under the same conditions.

Immobilization of His_6-ACP_6 was performed with an NTA chip (Biacore AB). The chip was coated with nickel ions by injection of $NiCl_2$ (500 μM, 20 μL) at a flow rate of 20 μL min^{-1}. His_6-ACP_6 (500 RU) was captured on the Ni-coated chip by injection of protein sample (200 nM) at a flow rate of 5 μL min^{-1} for 10 min. Kinetic analysis for the interaction of ACP_6 with untagged TE was carried out by injection of TE at different concentrations in running buffer (10 mM HEPES-KOH buffer (pH 7.4), 150 mM NaCl, 50 μM EDTA, 10 mM imidazole, and 0.005% P20 surfactant) at a flow rate of 10 μL min^{-1}

for 3 min. The experimental surface was regenerated by injection of regeneration solution (10 mM HEPES-KOH buffer (pH 7.4), 150 mM NaCl, 300 mM EDTA, and 0.005% P20 surfactant) at a flow rate of 20 $\mu L\,min^{-1}$ for 3 min. Untagged TE was also injected into a flow cell without immobilized His_6-ACP_6 to control for refractive index changes and nonspecific binding.

Immobilization of TE_6 was performed with a CM5 chip (Biacore AB). The chip was activated by injection of freshly prepared EDC (0.2 M) and NHS (0.05 M; 1:1, 200 μL) at a flow rate of 5 $\mu L\,min^{-1}$ at 25 °C. Anti-His_6 mAb (AbCam) was coupled to the chip by injection of protein (50 $\mu g\,mL^{-1}$) in sodium acetate buffer (10 mM, pH 4.0) for 3 min, followed by ethanolamine (1.0 M, 100 μL) to deactivate any remaining active ester sites. Anti-His_6 mAb (1000 RU) was immobilized on the CM5 surface. TE-His_6 was captured by flowing the domain over the chip at 50 $\mu g\,mL^{-1}$ in running buffer. Binding experiments were conducted by injection of ACP_6 at different concentrations in running buffer at a flow rate of 10 $\mu L\,min^{-1}$ for 3 min.

Data were analyzed with the aid of the BIAevaluation software package (Biacore AB).

Isothermal titration calorimetry: Calorimetric titrations were performed with PBS (50 mM NaPi (pH 8.0), 150 mM NaCl) in a MicroCal VP-ITC microcalorimeter. The sample cell of the calorimeter was filled with TE_{SA} mutant (0.1 mM) to a volume of 1.4 mL, and the system was allowed to equilibrate thermally at 20 °C. Pulses of the ligand solution (2 mM *apo-*, *holo-*, or butyryl-ACP_6, 10 μL) were then injected into the sample at 3 min intervals (it was not possible to increase the concentration of the ACP species further, due to limited solubility). Raw ITC data from two independent determinations were integrated by use of the Microcal Origin software, and background heats from ligand to buffer titrations were subtracted. The integrated heats for titration with butyryl-ACP_6 were fit to a single binding site model with stoichiometry set at 1:1.

Note Added in Proof

Recent crystallographic studies of the ECH2 decarboxylase CurF have shown that 20-fold discrimination against CoA-bound substrates is likely to arise from the presence in the active site of a tyrosine, which blocks a basic side chain of arginine from entering. In CoA-binding enzymes, this Arg interacts with both phosphate groups of CoA. Thus, in this case, discrimination is against the two phosphate groups of CoA in favor of the single phosphate group of the ACP-bound substrate. Such a mechanism might also be operative in the TE domain. T. W. Geders, L. Gu, J. C. Mowers, H. Liu, W. H. Gerwick, K. Håkansson, D. H. Sherman, J. L. Smith, *J. Biol. Chem.* **2007**, *282*, 35 954–35 963.

Acknowledgements

Bojana Popovic and Marko Hyvonen are thanked for help with isothermal titration calorimetry. L.T. was supported by Universities UK and the Cambridge Australia Trust; K.J.W. was supported by a Royal Society Dorothy Hodgkin Research Fellowship. We are grateful for the support of this work by the United Kingdom Biotechnology and Biological Sciences Research Council (BBSRC).

Keywords: acyl carrier proteins · biosynthesis · polyketides · protein structures · synthases · thioesterases

[1] K. J. Weissman, P. F. Leadlay, *Nat. Rev. Microbiol.* **2005**, *3*, 925–936.
[2] A. M. Hill, *Nat. Prod. Rep.* **2006**, *23*, 256–320.
[3] C. Hertweck, A. Luzhetskyy, Y. Rebets, A. Bechthold, *Nat. Prod. Rep.* **2007**, *24*, 162–190.
[4] S. Smith, A. Witkowski, A. K. Joshi, *Prog. Lipid Res.* **2003**, *42*, 289–317.
[5] J. Cortés, S. F. Haydock, G. A. Roberts, D. J. Bevitt, P. F. Leadley, *Nature* **1990**, *348*, 176–178.
[6] S. Donadio, M. J. Staver, J. B. McAlpine, S. J. Swanson, L. Katz, *Science* **1991**, *252*, 675–679.
[7] H. G. Floss, *J. Biotechnol.* **2006**, *124*, 242–257.
[8] M. P. Crump, J. Crosby, C. E. Dempsey, J. A. Parkinson, M. Murray, D. A. Hopwood, T. J. Simpson, *Biochemistry* **1997**, *36*, 6000–6008.
[9] G. Y. Xu, A. Tam, L. Lin, J. Hixon, C. C. Fritz, R. Powers, *Structure* **2001**, *9*, 277–287.
[10] H. C. Wong, G. Liu, Y. M. Zhang, C. O. Rock, J. Zheng, *J. Biol. Chem.* **2002**, *277*, 15874–15880.
[11] S. C. Findlow, C. Winsor, T. J. Simpson, J. Crosby, M. P. Crump, *Biochemistry* **2003**, *42*, 8423–8433.
[12] A. K. Sharma, S. K. Sharma, A. Surolia, N. Surolia, S. P. Sarma, *Biochemistry* **2006**, *45*, 6904–6916.
[13] V. Y. Alekseyev, C. W. Liu, D. E. Cane, J. D. Puglisi, C. Khosla, *Protein Sci.* **2007**, *16*, 2093–2107.
[14] Y. M. Zhang, B. Wu, J. Zheng, C. O. Rock, *J. Biol. Chem.* **2003**, *278*, 52935–52943.
[15] Y. M. Zhang, H. Marrakchi, S. W. White, C. O. Rock, *J. Lipid Res.* **2003**, *44*, 1–10.
[16] L. M. Worsham, L. Earls, C. Jolly, K. G. Langston, M. S. Trent, M. L. Ernst-Fonberg, *Biochemistry* **2003**, *42*, 167–176.
[17] Y. M. Zhang, M. S. Rao, R. J. Heath, A. C. Price, A. J. Olson, C. O. Rock, S. W. White, *J. Biol. Chem.* **2001**, *276*, 8231–8238.
[18] A. T. Hadfield, C. Limpkin, W. Teartasin, T. J. Simpson, J. Crosby, M. P. Crump, *Structure* **2004**, *12*, 1865–1875.
[19] C. Khosla, S. Ebert-Khosla, D. A. Hopwood, *Mol. Microbiol.* **1992**, *6*, 3237–3249.
[20] C. Khosla, R. McDaniel, S. Ebert-Khosla, R. Torres, D. H. Sherman, M. J. Bibb, D. A. Hopwood, *J. Bacteriol.* **1993**, *175*, 2197–2204.
[21] T. S. Lee, C. Khosla, Y. Tang, *J. Am. Chem. Soc.* **2005**, *127*, 12254–12262.
[22] K. J. Weissman, H. Hong, B. Popovic, F. Meersman, *Chem. Biol.* **2006**, *13*, 625–636.
[23] K. J. Weissman, H. Hong, M. Oliynyk, A. P. Siskos, P. F. Leadlay, *ChemBioChem* **2004**, *5*, 116–125.
[24] R. H. Lambalot, A. M. Gehring, R. S. Flugel, P. Zuber, M. LaCelle, M. A. Marahiel, R. Reid, C. Khosla, C. T. Walsh, *Chem. Biol.* **1996**, *3*, 923–936.
[25] Y. Tang, A. Y. Chen, C. Y. Kim, D. E. Cane, C. Khosla, *Chem. Biol.* **2007**, *14*, 931–943.
[26] G. Yadav, R. S. Gokhale, D. Mohanty, *Nucleic Acids Res.* **2003**, *31*, 3654–3658.
[27] S. C. Tsai, L. J. Miercke, J. Krucinski, R. Gokhale, J. C. Chen, P. G. Foster, D. E. Cane, C. Khosla, R. M. Stroud, *Proc. Natl. Acad. Sci. USA* **2001**, *98*, 14808–14813.
[28] P. Caffrey, B. Green, L. C. Packman, B. J. Rawlings, J. Staunton, P. F. Leadlay, *Eur. J. Biochem.* **1991**, *195*, 823–830.
[29] K. J. Weissman, C. J. Smith, U. Hanefeld, R. Aggarwal, M. Bycroft, J. Staunton, P. F. Leadlay, *Angew. Chem.* **1998**, *110*, 1503–1506; *Angew. Chem. Int. Ed.* **1998**, *37*, 1437–1440.
[30] R. Aggarwal, P. Caffrey, P. F. Leadlay, C. J. Smith, J. Staunton, *J. Chem. Soc. Chem. Commun.* **1995**, 1519–1520.
[31] N. Wu, D. E. Cane, C. Khosla, *Biochemistry* **2002**, *41*, 5056–5066.
[32] L. E. Quadri, P. H. Weinreb, M. Lei, M. M. Nakano, P. Zuber, C. T. Walsh, *Biochemistry* **1998**, *37*, 1585–1595.
[33] R. S. Gokhale, D. Hunziker, D. E. Cane, C. Khosla, *Chem. Biol.* **1999**, *6*, 117–125.
[34] J. Cortés, K. E. H. Wiesmann, G. A. Roberts, M. J. Brown, J. Staunton, P. F. Leadlay, *Science* **1995**, *268*, 1487–1489.
[35] G. L. Ellman, *Arch. Biochem. Biophys.* **1959**, *82*, 70–77.
[36] P. A. van der Merwe in *Protein–Ligand Interactions: A Practical Approach, Vol. 1: Hydrodynamics and Calorimetry* (Eds.: S. Harding, P. Z. Chowdhry), Oxford University Press, Oxford **2001**, pp. 137–170.
[37] M. L. Doyle in *Quantitation of Protein Interactions* (Ed.: V. Chanda), Wiley, New York **1999**, pp. 20.4.1–20.4.24.
[38] S. J. Moss, C. J. Martin, B. Wilkinson, *Nat. Prod. Rep.* **2004**, *21*, 575–593.

[39] B. Wilkinson, G. Foster, B. A. Rudd, N. L. Taylor, A. P. Blackaby, P. J. Sidebottom, D. J. Cooper, M. J. Dawson, A. D. Buss, S. Gaisser, I. U. Böhm, C. J. Rowe, J. Cortés, P. F. Leadlay, J. Staunton, *Chem. Biol.* **2000**, *7*, 111–117.
[40] C. D. Richter, D. A. Stanmore, R. N. Miguel, M. C. Moncrieffe, L. Tran, S. Brewerton, F. Meersman, R. W. Broadhurst, K. J. Weissman, *FEBS J.* **2007**, *274*, 2196–2209.
[41] Y. Tang, C. Y. Kim, I. I. Mathews, D. E. Cane, C. Khosla, *Proc. Natl. Acad. Sci. USA* **2006**, *103*, 11124–11129.
[42] A. T. Keatinge-Clay, R. M. Stroud, *Structure* **2006**, *14*, 737–748.
[43] R. N. Perham, *Annu. Rev. Biochem.* **2000**, *69*, 961–1004.
[44] H. Hong, A. N. Appleyard, A. P. Siskos, J. Garcia-Bernardo, J. Staunton, P. F. Leadlay, *FEBS J.* **2005**, *272*, 2373–2387.
[45] A. K. Joshi, A. Witkowski, H. A. Berman, L. Zhang, S. Smith, *Biochemistry* **2005**, *44*, 4100–4107.
[46] J. S. Mattick, J. Nickless, M. Mizugaki, C. Y. Yang, S. Uchiyama, S. J. Wakil, *J. Biol. Chem.* **1983**, *258*, 15 300–15 304.
[47] A. C. Mercer, M. D. Burkart, *Nat. Prod. Rep.* **2007**, *24*, 750–773.
[48] Q. Li, C. Khosla, J. D. Puglisi, C. W. Liu, *Biochemistry* **2003**, *42*, 4648–4657.
[49] A. Roujeinikova, C. Baldock, W. J. Simon, J. Gilroy, P. J. Baker, A. R. Stuitje, D. W. Rice, A. R. Slabas, J. B. Rafferty, *Structure* **2002**, *10*, 825–835.
[50] Z. A. Hughes-Thomas, C. B. Stark, I. U. Böhm, J. Staunton, P. F. Leadlay, *Angew. Chem.* **2003**, *115*, 4613–4616; *Angew. Chem. Int. Ed.* **2003**, *42*, 4475–4478.
[51] C. J. Martin, M. C. Timoney, R. M. Sheridan, S. G. Kendrew, B. Wilkinson, J. Staunton, P. F. Leadlay, *Org. Biomol. Chem.* **2003**, *1*, 4144–4147.
[52] J. W. Giraldes, D. L. Akey, J. D. Kittendorf, D. H. Sherman, J. L. Smith, R. A. Fecik, *Nat. Chem. Biol.* **2006**, *2*, 531–536.
[53] D. L. Akey, J. D. Kittendorf, J. W. Giraldes, R. A. Fecik, D. H. Sherman, J. L. Smith, *Nat. Chem. Biol.* **2006**, *2*, 537–542.
[54] A. Y. Chen, D. E. Cane, C. Khosla, *Chem. Biol.* **2007**, *14*, 784–792.

Received: December 6, 2007
Published online on March 17, 2008

